26th AIAA Applied Aerodynamics Conference
18 - 21 August 2008, Honolulu, Hawaii

AIAA 2008-6246

Static Testing of Micro Propellers

Robert W. Deters* and Michael S. Selig †
University of Illinois at Urbana-Champaign, Urbana, Illinois 61801

Available performance data for micro propellers are very lacking. Prediction of micro propeller performance is made difficult due to the small Reynolds numbers (less than 50,000) at which the propellers operate. A test rig was designed and built at the University of Illinois at Urbana-Champaign in order to measure the static performance of micro propellers. A load cell and torque transducer measure the thrust and torque, respectively, created by a propeller. These results are then used to find the static thrust and power coefficients. Eighteen two-bladed propellers from different manufacturers and two three-bladed propellers were tested with diameters ranging from 2.25 in. to 5 in. The hovering capabilities of the propellers were also analyzed.

I. Introduction

Small scale propellers have been widely used for radio controlled (RC) aircraft. The size and shape of the propellers used vary just as much as the type of RC aircraft flown. A large number of ready-to-fly RC aircraft are now available, many of which are constructed of foam. These aircraft are fairly inexpensive and use small motors and propellers with diameters less than 5 in. to provide thrust. An increased interest in Micro Air Vehicles (MAVs) in industry and for the military creates a need for data on micro propellers as well. Experimental data on these micro propellers are lacking and predicting static data is difficult due to the very low Reynolds numbers that these propellers experience (less than 50,000). Knowing the static performance of micro propellers would be very useful in determining motor selection and flight capabilities of small RC aircraft. This information would be very helpful for planes that can perform the prop-hanging maneuver. During prop-hanging, the fuselage is vertical and the propeller is providing enough thrust to keep the aircraft in the air. This maneuver gives the illusion that the aircraft is "hanging" on the propeller.

Previous work has been done on small scale propellers at the University of Illinois at Urbana-Champaign[1–4] and at Wichita State University.[5] Tests from Wichita are for propellers ranging from 6 to 22 in. Most tests at Illinois have been done on propellers with a diameter ranging from 9 to 11 in., but a limited number of larger propellers and propellers down to 6 in. have also been tested. The test rig at Illinois for these propellers can test both static performance and propeller performance in a moving air flow. This test rig was not designed to test micro propellers, so a new test rig, used in the current tests, was built. Since only static performance was sought, the new rig was not designed to be installed in a wind tunnel.

II. Experimental Setup

Thrust, torque, and propeller speed were all measured using the experimental test rig shown schematically in Fig 1. Propeller thrust was measured using the SSP1-0.3KG load cell maufactured by Load Cell Central. The load cell has a capacity of 10.58 oz (0.3 kg). Torque was measured using the RTS-25 reaction torque transducer manufactured by Transducer Techniques. The torque transducer has a capacity of 25 oz-in. Propeller speed ranged from 2,500 RPM up to 27,000 RPM, and was measured using a matched infrared emitter and phototransistor detector stationed so that the propeller blades would pass between them. The atmospheric pressure was measured using a MKS absolute pressure transducer, and the air temperature was measured with an Omega GRMQSS T-type thermocouple.

*Graduate Research Assistant, Department of Aerospace Engineering, rdeters@illinois.edu, and AIAA Student Member.
†Associate Professor, Department of Aerospace Engineering, m-selig@illinois.edu, and AIAA Senior Member.

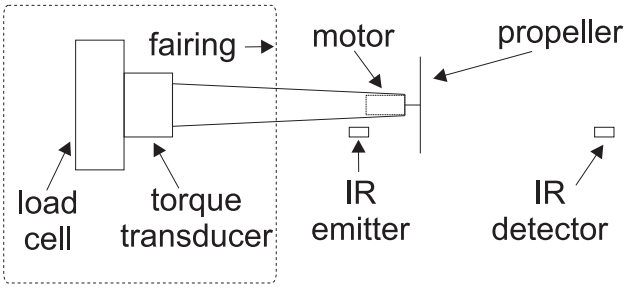

Figure 1. Schematic of the experimental test rig viewed from the side.

A Medusa MR-012-030-4000 brushless motor was used for the tests. The motor was attached to a mount, which in turn was attached directly to the torque transducer. The torque transducer was attached to the thrust load cell, and the load cell was attached to the rig support. In order to isolate the load cell and torque transducer from the prop wash, an airfoil shaped fairing was installed. Since the motor was brushless, it was attached to a Castle Creations Thunderbird-9 speed controller. To supply power for the motor and speed controller, a power supply made by BK Precision was used. Between the power supply and the speed controller, an E-flite power meter was connected to monitor amperage in order to not overload the motor. To set the rotational speed of the motor, the speed controller was connected to the ServoXciter EF made by Vexa Control. This device was used to act like a throttle. The data acquisition software was set up to control the motor by changing the voltage sent to the ServoXciter.

Voltages from the torque transducer and load cell were recorded by a National Instruments analog-to-digital data acquisition board connected to a personal computer. Voltages were converted to thrust and torque using calibration slopes. Thrust calibration used precisely measured weights to pull on the motor when it was attached to the test rig. By increasing and decreasing the amount of force on the test rig, a linear relationship between the voltage and the force was found. Torque calibration was done by using the weights and a moment arm to generate a known torque on the torque transducer. A linear relationship between the voltages and the torque was found. These calibrations were performed regularly to ensure consistent results.

The purpose of these propeller tests was to find the thrust and torque produced at given propeller RPMs. The first part of each test was to determine the RPM range for a propeller. The data acquisition software has a tool that allows the user to manually set the voltage sent to the ServoXciter and displays the resulting RPM. The upper RPM limit was set so that the amperage and power being used by the motor was safely below the manufacturer's limits. The second part of the test was the actual testing phase. The data acquisition software sent a voltage to the ServoXciter that in turn sent a signal to the speed control. The resulting RPM was measured by the infrared emitter-detector pair. The software then increased or decreased the voltage to the ServoXciter in order to set the RPM to the lower RPM limit. Thrust and torque measurements were taken along with the current ambient pressure and temperature. The software then set the next propeller RPM and more data were recorded. This continued until the upper RPM limit was reached.

The data acquisition software also reduced the data to produce thrust and power coefficients. Air density was calculated by

$$\rho = \frac{P_{atm}}{R T_{air}} \tag{1}$$

Propeller power was calculated by

$$P = 2\pi n Q \tag{2}$$

where Q is the propeller torque and n is the propeller rotational speed measured in revolutions per second. The thrust and power coefficients were then calculated by

$$C_{T_0} = \frac{T_0}{\rho\, n^2 D^4} \tag{3}$$

$$C_{P_0} = \frac{P_0}{\rho\, n^3 D^5} \tag{4}$$

where D is the diameter of the propeller.

Geometry for each propeller was also found. Using an image of the front and side of each propeller, the PropellerScanner software from MH Aero found the chord and twist distribution.[6]

In order to be able to compare the static performance of the different propellers, a static efficiency was calculated. This efficiency was in the form of the hover figure of merit or FOM.[7,8] Usually used to measure the efficiency of helicopter rotors, FOM is the ratio of the ideal power required to hover to the actual power required, or

$$FOM = \frac{P_{ideal}}{P} \tag{5}$$

From momentum theory, the ideal power is given as

$$P_{ideal} = T\sqrt{T/2\rho A} \tag{6}$$

so FOM becomes

$$FOM = \frac{C_T^{3/2}}{\sqrt{2}\, C_P} \tag{7}$$

The thrust and power coefficients used in Eqn. 7 are defined slightly different than those shown in Eqns. 3–4. The FOM equation is typically used for helicopters, so the thrust and power coefficients are defined as

$$C_T = \frac{T_0}{\rho A V_T^2} \tag{8}$$

$$C_P = \frac{P_0}{\rho A V_T^3} \tag{9}$$

where A is the disk area and V_T is the tip speed. The FOM values found in this report use the coefficient definitions shown in Eqns. 8–9. Care must be taken when using the FOM to compare rotors. Only rotors with the same disk loading should be compared.

III. Results

Twenty propellers were tested with diameters ranging from 2.25 in. to 5 in. (Figs. 2–7). Ten propellers were manufactured by GWS and are shown in Figs. 2 and 3. These propellers range in diameter from 2.5 in. to 5 in. Five propellers were manufactured by Micro Invent and range in diameter from 3.2 in. to 5 in. Three of the Micro Invent propellers had 2 blades (Fig. 4) while the other two had 3 blades (Fig. 5). Three propellers were from Plantraco (Fig. 6) and range in diameter from 2.25 in. to 4 in. Of the last two propellers shown in Fig. 7, one was from Union with a diameter of 3.15 in. and the other was a folding propeller from KP Aero Models with a diameter of 3.8 in.

All of the propellers tested had thin cross sections and all but five were made of plastic. The five Micro Invent propellers were all made of carbon laminate. These propellers had thinner cross sections than the plastic propellers and were more flexible. This extra flexibility led to significant blade twisting during testing, and it is believed that this twisting reduced the propeller pitch. The GWS propellers used a very thin flat-bottom airfoil while the other propellers were thin foil surfaces.

The geometry and static performance data of each propeller can be found in Figs. 8–67. The GWS propellers are shown in Figs. 8–37, the Micro Invent propellers are shown in Figs. 38–52, the Plantraco propellers are shown in Figs. 53–61, the Union propeller is shown in Figs. 62–64, and the KP propeller is shown in Figs. 65–67. Each propeller data set includes three figures. The first figure shows the chord and twist distribution from PropellerScanner along with pictures of the propeller from the top and side. The other two figures show the static performance in the form of static thrust and power coefficients plotted against RPM. The Reynolds numbers of the propellers are also shown in the static performance plots, and it is seen that the propellers operate at values less than 50,000. The Reynolds numbers are based on the chord at the 75% blade station.

A table of the propellers tested and some important information is shown in Table 1. This table provides the RPM range at which each propeller was tested along with the disk loading (T/A). The FOM for each

Figure 2. GWS Direct Drive propellers with diameters ranging from 2.5 in. to 4.0 in.

Figure 3. GWS Direct Drive propellers with diameters of 4.5 in. and 5.0 in.

propeller is also given. The FOM for a typical rotor will increase as the thrust coefficient increases until it reaches a peak and stays fairly constant. At the RPM range these propellers were tested, the FOM had already reached its peak. Therefore the FOM shown in the table is an average over the RPM range. Since all of the propellers share some common range in disk loading, the FOM can be used to make some comparisons.

An efficient rotor typically has a FOM between 0.7 and 0.8, but as seen in the table, these propellers do not reach this high of a value. This is not surprising since these propellers were not designed for hovering. A couple of trends can be seen from the FOM results. A larger diameter propeller tends to be more efficient, and for propellers of the same diameter, a lower pitch tends to be more efficient.

IV. Summary

Static tests of twenty off-the-shelf propellers were performed. Thrust and torque data was measured and thrust and power coefficients were calculated. Using top and side-view pictures of the propellers, the chord and twist distributions were found. To better compare the static performance of the propellers, a figure of merit was calculated. The results have shown that propellers with a larger diameter were typically more efficient, and lower pitch for propellers of the same diameter were more efficient. The results of these twenty propeller provide a set of available data that can be used to compare against static performance prediction codes.

Table 1. Summary Data and Figure of Merit for the Twenty Propellers Tested

Manufacturer	Propeller	Diameter (in)	RPM low	RPM high	T/A low (lb/ft^2)	T/A high (lb/ft^2)	FOM
GWS	2.5×0.8	2.55	15,000	27,000	0.49	1.62	0.382
	2.5×1.0	2.55	15,000	27,000	0.61	1.98	0.440
	3.0×2.0	3.25	7,000	18,000	0.37	2.57	0.531
	3.0×3.0	3.20	5,000	16,000	0.26	2.75	0.455
	4.0×2.5	4.00	5,000	15,000	0.26	2.46	0.572
	4.0×4.0	4.00	4,000	11,000	0.23	1.76	0.419
	4.5×3.0	4.50	4,000	12,000	0.20	1.93	0.556
	4.5×4.0	4.50	3,000	10,000	0.15	1.71	0.526
	5.0×3.0	5.00	3,000	10,000	0.13	1.60	0.611
	5.0×4.3	5.00	2,500	8,500	0.13	1.46	0.562
Micro Invent	3.2×2.2	3.20	9,000	19,000	0.55	2.57	0.524
	4.0×2.7	3.95	6,000	13,000	0.30	1.66	0.418
	5.0×3.5	4.90	4,000	8,000	0.20	0.96	0.582
	4.3×3.5T	4.40	4,000	9,000	0.25	1.49	0.545
	5.0×4.0T	4.90	3,000	7,000	0.18	1.13	0.480
Plantraco	57 mm × 20 mm	2.25	12,000	24,000	0.54	2.32	0.437
	Tri-Turbofan	2.55	9,000	20,000	0.49	2.47	0.438
	100 mm	4.00	5,000	12,000	0.28	1.75	0.415
Union	U-80	3.15	7,500	20,000	0.43	3.58	0.552
KP	96 mm Folding	3.80	4,000	11,000	0.25	1.93	0.490

Figure 4. Micro Invent propellers with diameters ranging from 3.2 in. to 5.0 in.

Acknowledgments

The authors wish to thank John Brandt for designing the original propeller acquisition software. Thanks also goes to Nathan Bishop for his initial work on this project. The authors also thank Craig Golema of Spin Master for providing the funding for these tests.

References

[1]Brandt, J., *Small-Scale Propeller Performance at Low Speeds*, M.S. Thesis, University of Illinois at Urbana-Champaign, Urbana, IL, 2005.

[2]Tehrani, K., *Propellers in Yaw at Low Speeds*, M.S. Thesis, University of Illinois at Urbana-Champaign, Urbana, IL, 2006.

[3]Uhlig, D.V., *Post Stall Propeller Behavior at Low Reynolds Numbers*, M.S. Thesis, University of Illinois at Urbana-Champaign, Urbana, IL, 2007.

[4]Uhlig, D.V. and Selig, M.S., "Post Stall Propeller Behavior at Low Reynolds Numbers," 46th Aerospace Sciences Meeting, AIAA Paper 2008-407, Jan. 2008.

[5]Merchant, M.P. and Miller, L.S., "Propeller Performance Measurement for Low Reynolds Number UAV Applications," 44th Aerospace Sciences Meeting, AIAA Paper 2006-1127, Jan. 2006.

[6]Hepperle, M., *PropellerScanner Manual*, www.mh-aerotools.de, 2003.

[7]Johnson, W., *Helicopter Theory*, Dover Publications, Inc., New York, 1980.

[8]Leishman, J.G., *Principles of Helicopter Aerodynamics*, Cambridge University Press, Cambridge, 2000.

Figure 5. Micro Invent 3-bladed propellers with diameters of 4.3 in. and 5.0 in.

Figure 6. Plantraco propellers with diameters ranging from 2.25 in. to 4.0 in.

Figure 7. Union propeller with a diameter of 3.15 in. and KP Aero Models propeller with a diameter of 3.8 in.

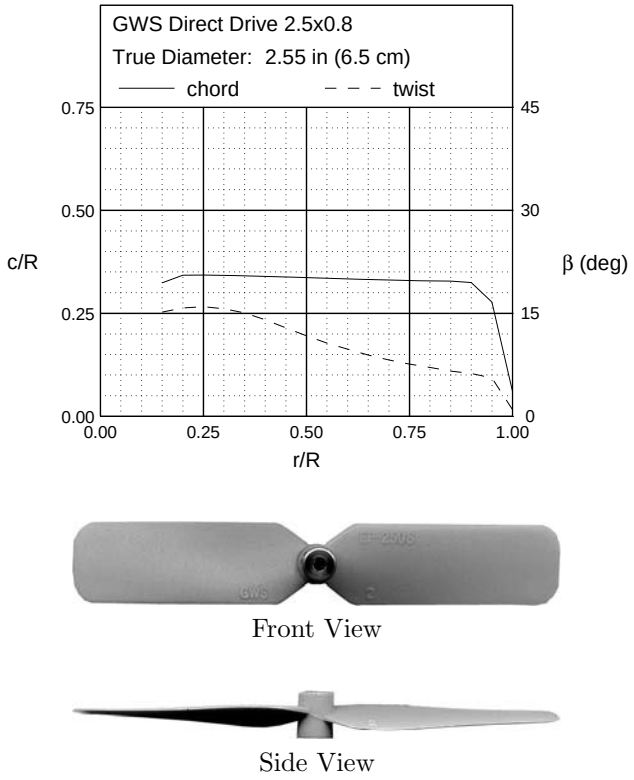

Figure 8. GWS Direct Drive 2.5×0.8 geometric characteristics.

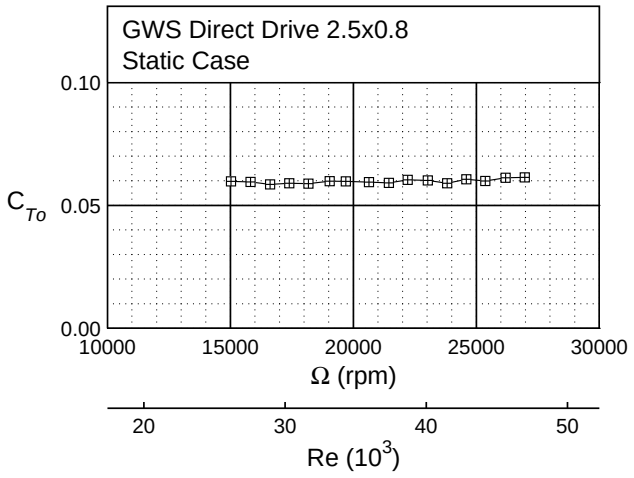

Figure 9. GWS Direct Drive 2.5×0.8 static thrust.

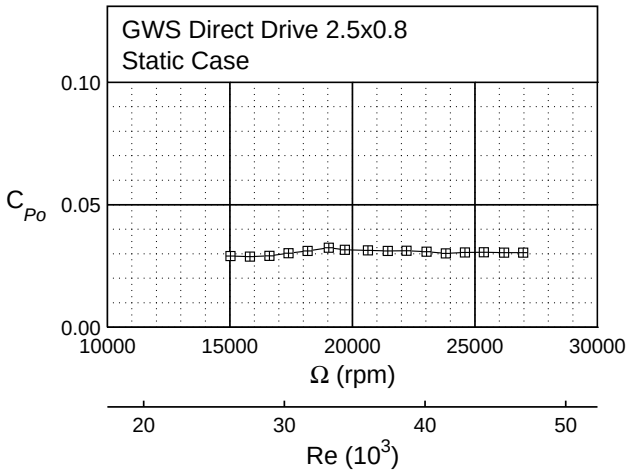

Figure 10. GWS Direct Drive 2.5×0.8 static power.

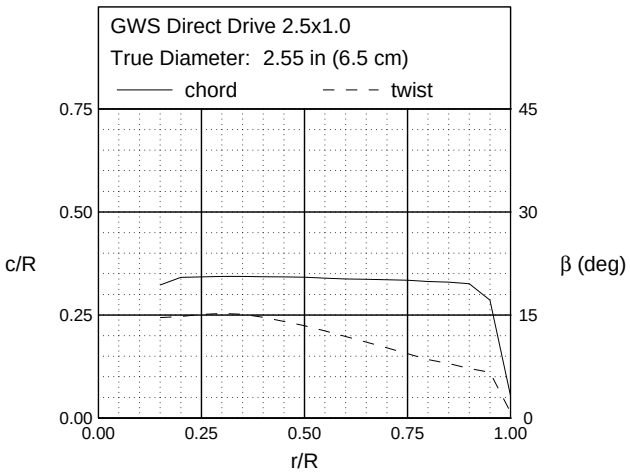

Front View

Side View

Figure 11. GWS Direct Drive 2.5×1.0 geometric characteristics.

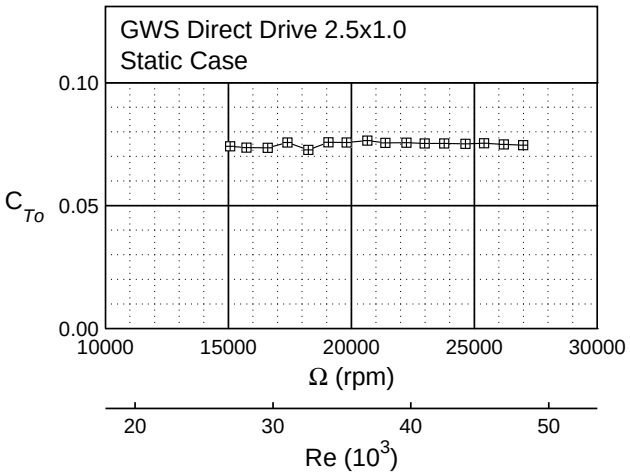

Figure 12. GWS Direct Drive 2.5×1.0 static thrust.

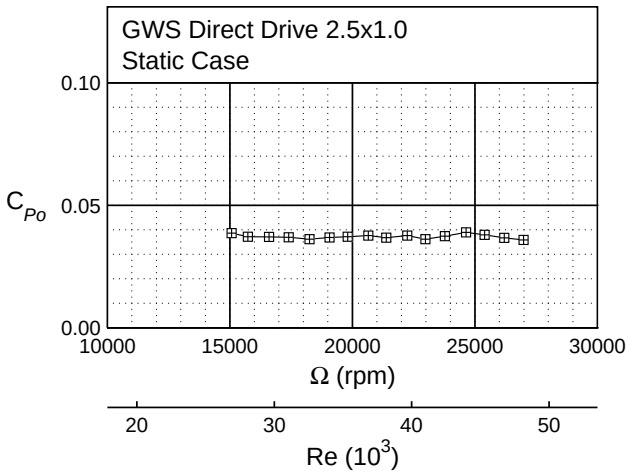

Figure 13. GWS Direct Drive 2.5×1.0 static power.

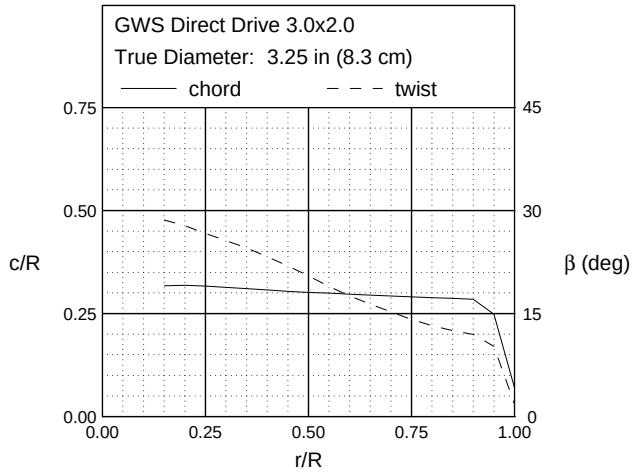

Front View

Side View

Figure 14. GWS Direct Drive 3.0×2.0 geometric characteristics.

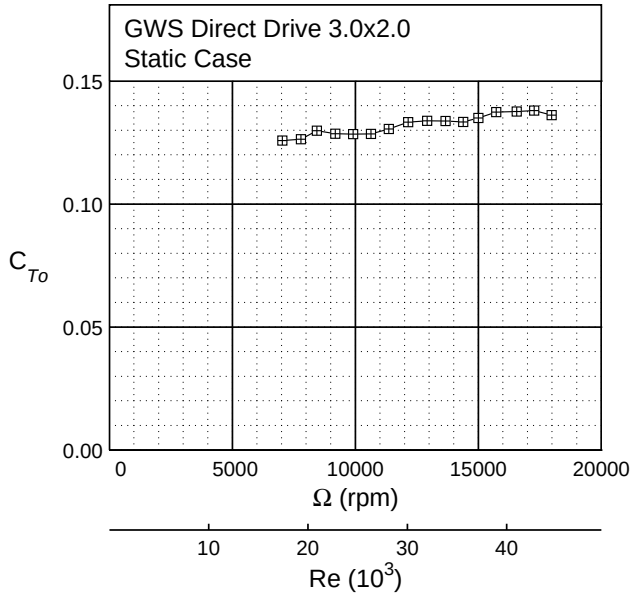

Figure 15. GWS Direct Drive 3.0×2.0 static thrust.

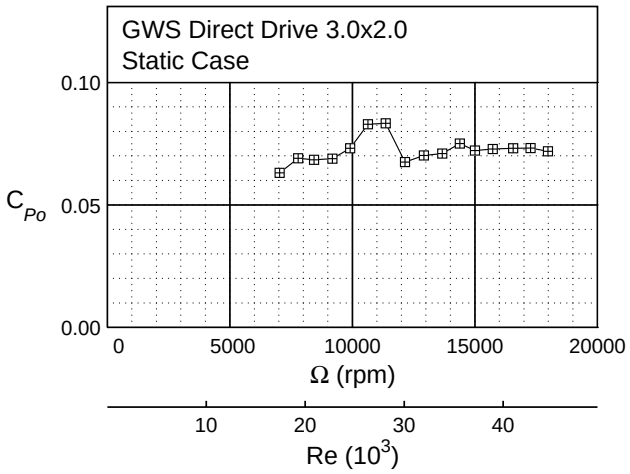

Figure 16. GWS Direct Drive 3.0×2.0 static power.

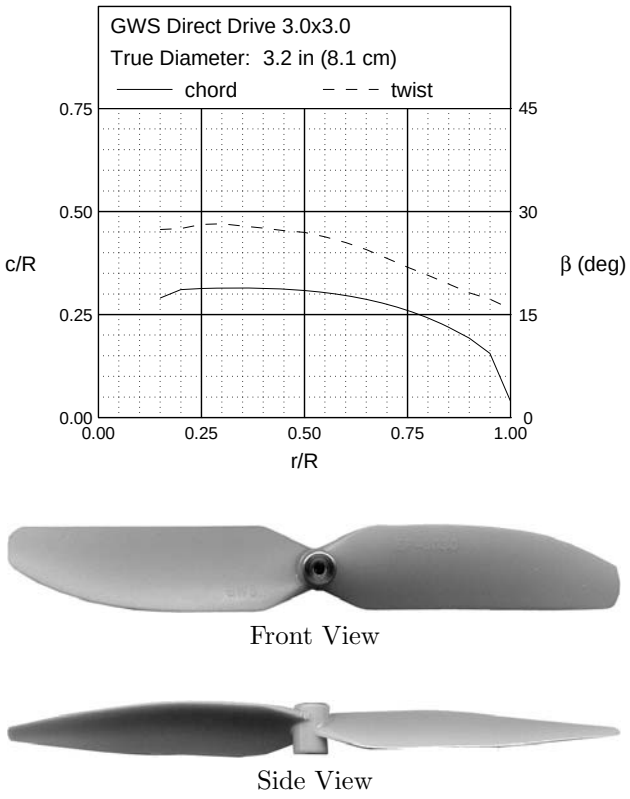

Figure 17. GWS Direct Drive 3.0×3.0 geometric characteristics.

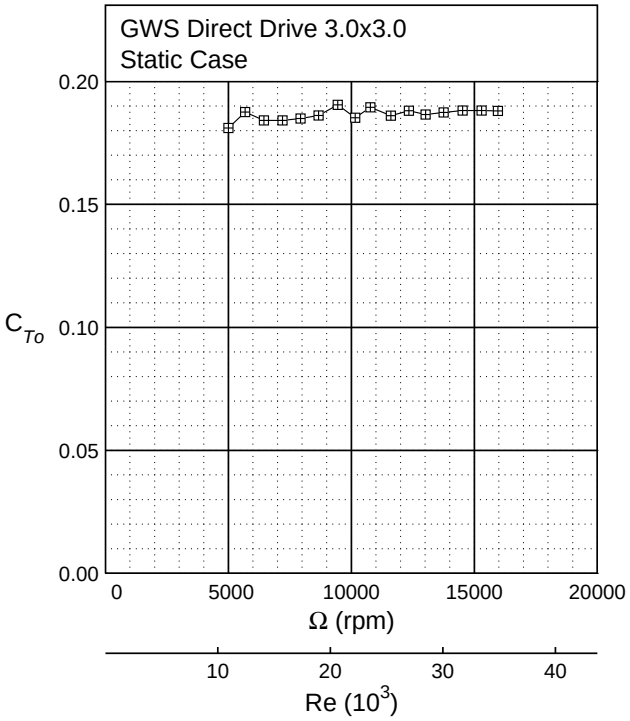

Figure 18. GWS Direct Drive 3.0×3.0 static thrust.

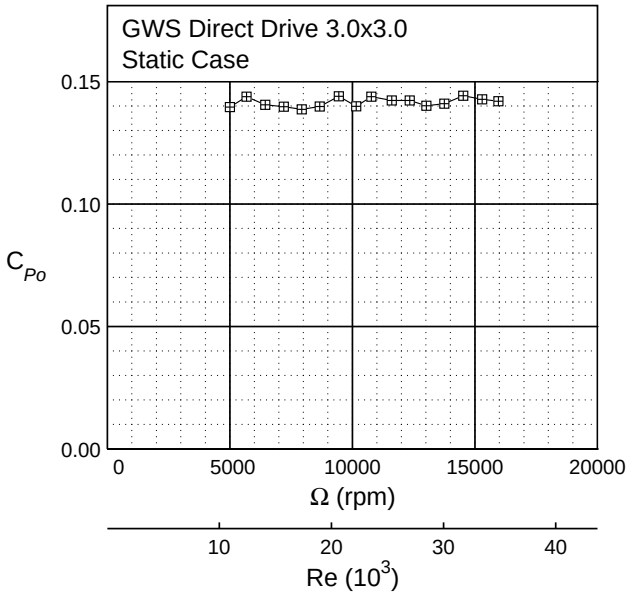

Figure 19. GWS Direct Drive 3.0×3.0 static power.

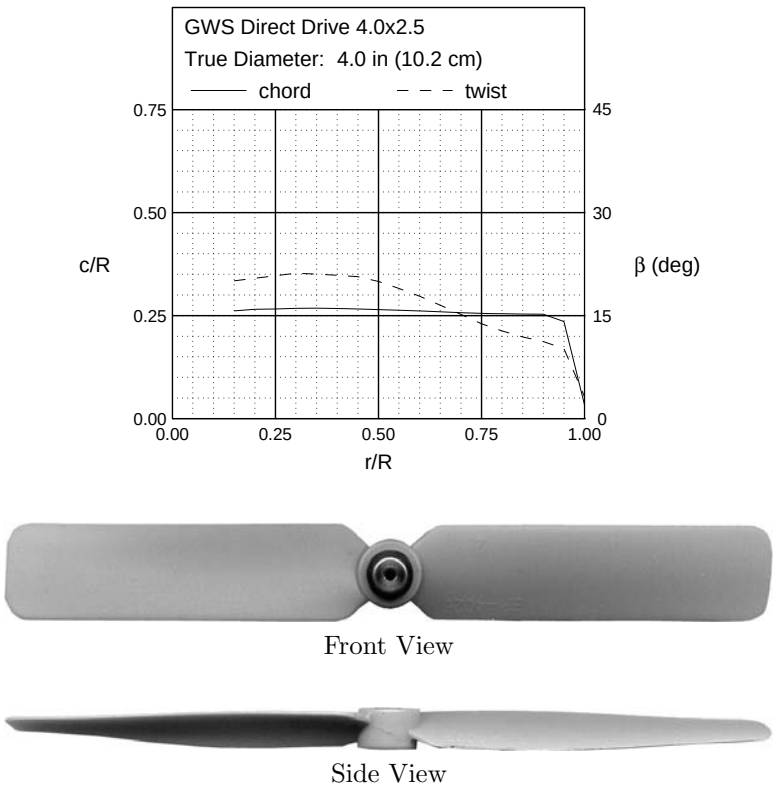

Figure 20. GWS Direct Drive 4.0×2.5 geometric characteristics.

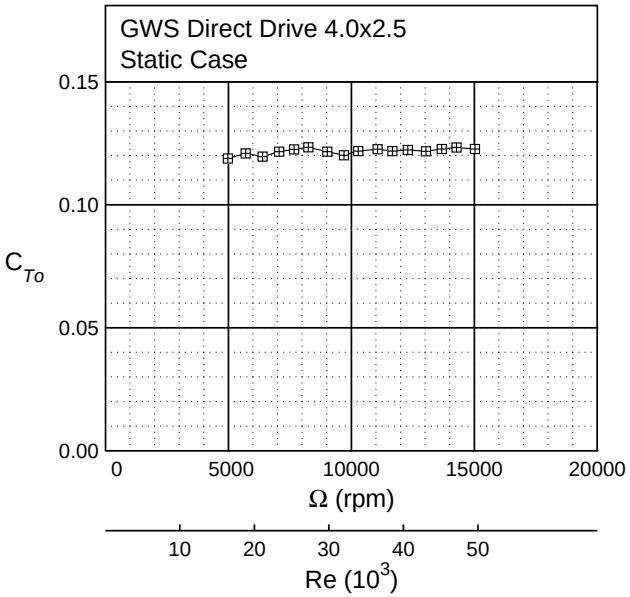

Figure 21. GWS Direct Drive 4.0×2.5 static thrust.

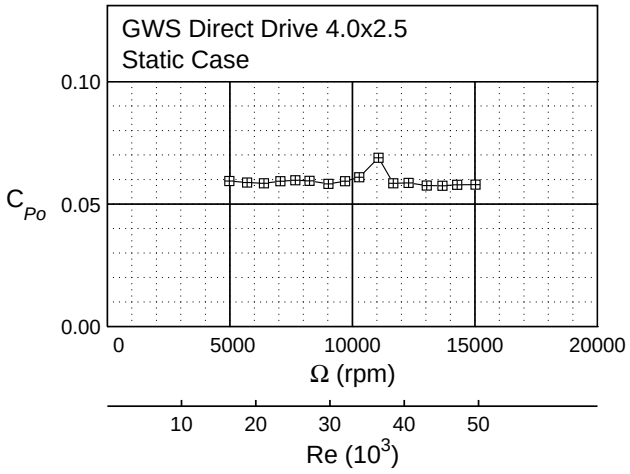

Figure 22. GWS Direct Drive 4.0×2.5 static power.

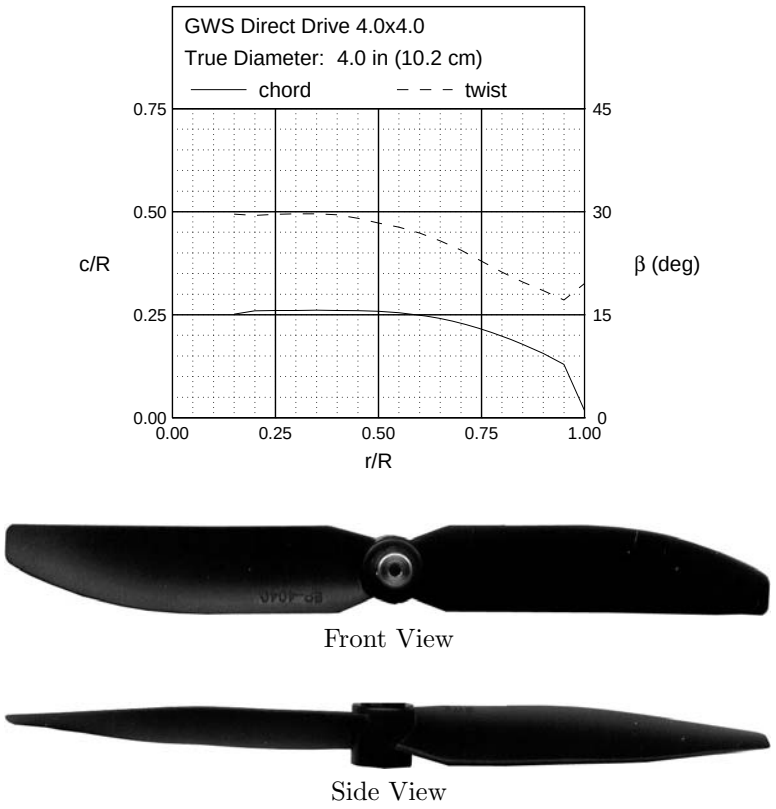

Figure 23. GWS Direct Drive 4.0×4.0 geometric characteristics.

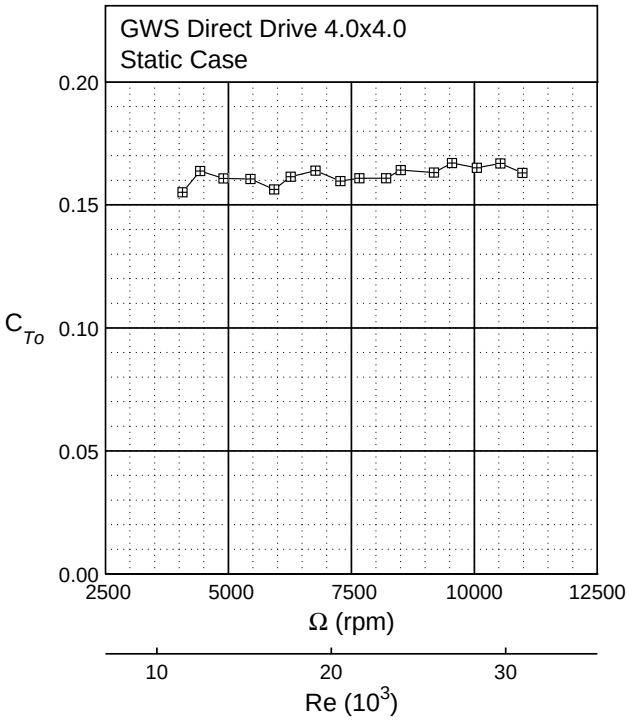

Figure 24. GWS Direct Drive 4.0×4.0 static thrust.

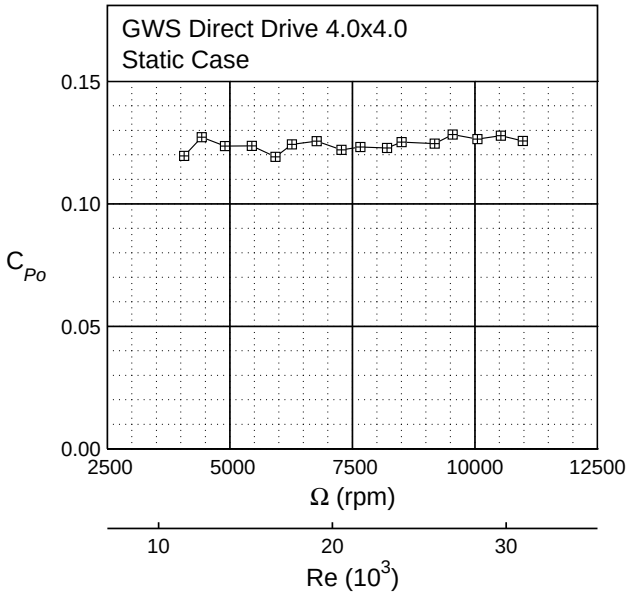

Figure 25. GWS Direct Drive 4.0×4.0 static power.

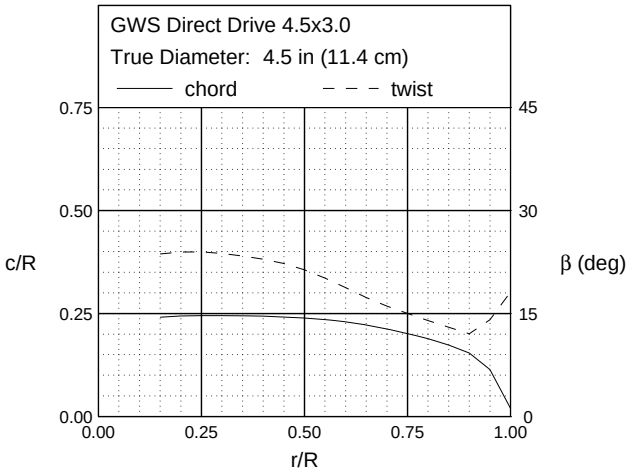

Front View

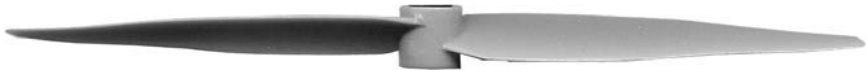

Side View

Figure 26. GWS Direct Drive 4.5×3.0 geometric characteristics.

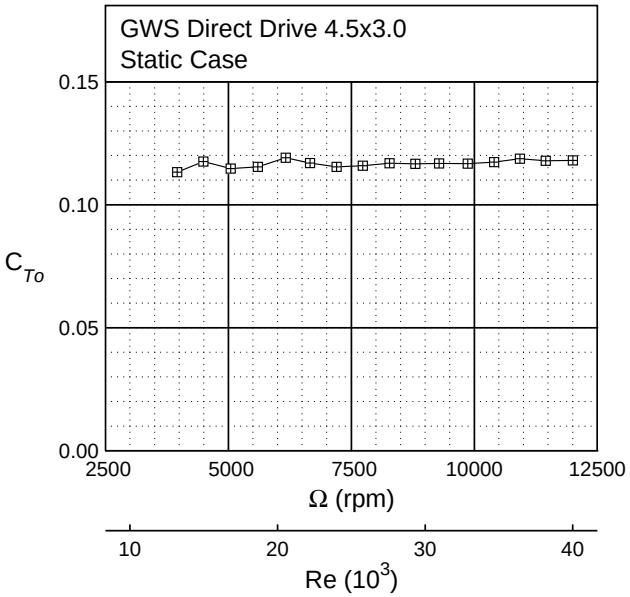

Figure 27. GWS Direct Drive 4.5×3.0 static thrust.

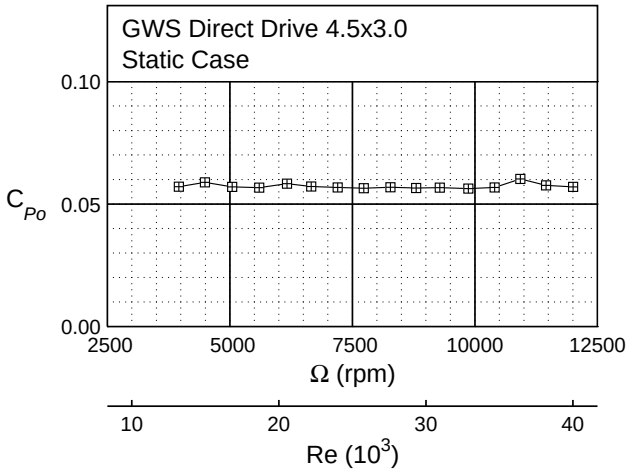

Figure 28. GWS Direct Drive 4.5×3.0 static power.

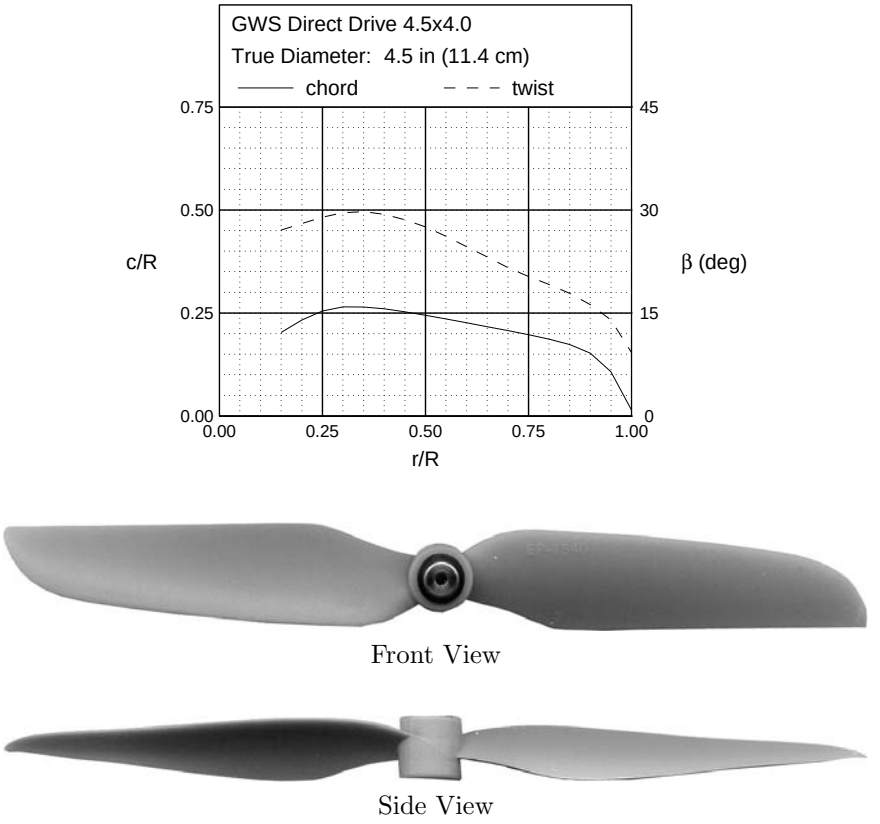

Figure 29. GWS Direct Drive 4.5×4.0 geometric characteristics.

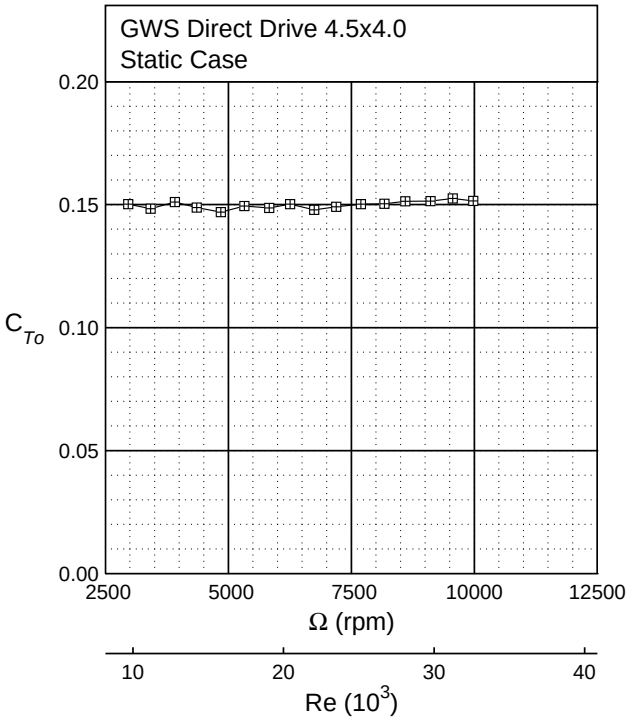

Figure 30. GWS Direct Drive 4.5×4.0 static thrust.

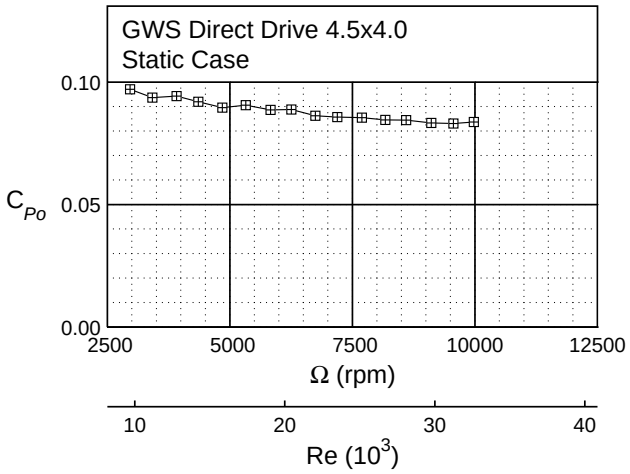

Figure 31. GWS Direct Drive 4.5×40 static power.

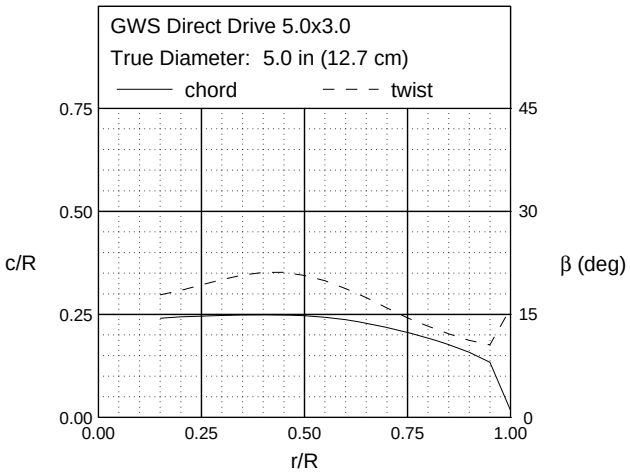

Front View

Side View

Figure 32. GWS Direct Drive 5.0×3.0 geometric characteristics.

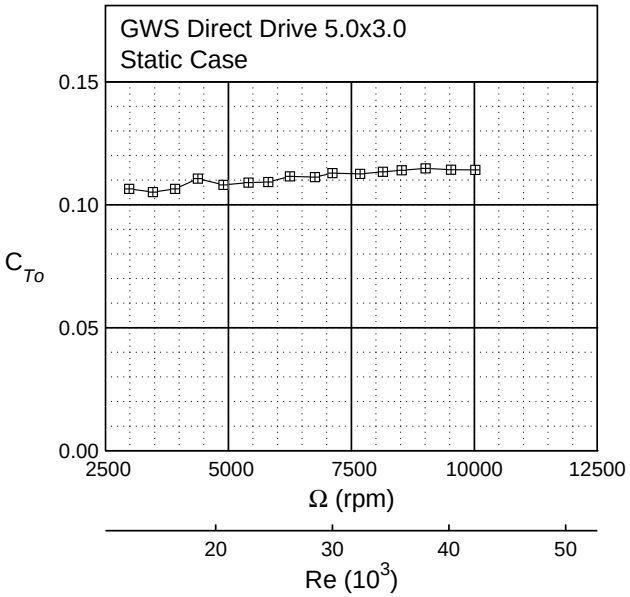

Figure 33. GWS Direct Drive 5.0×3.0 static thrust.

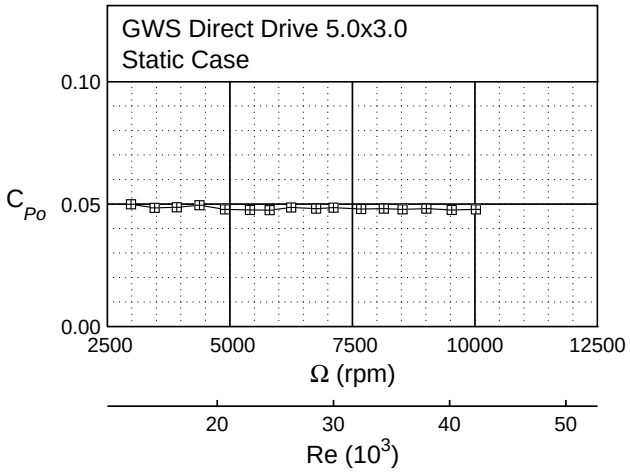

Figure 34. GWS Direct Drive 5.0×3.0 static power.

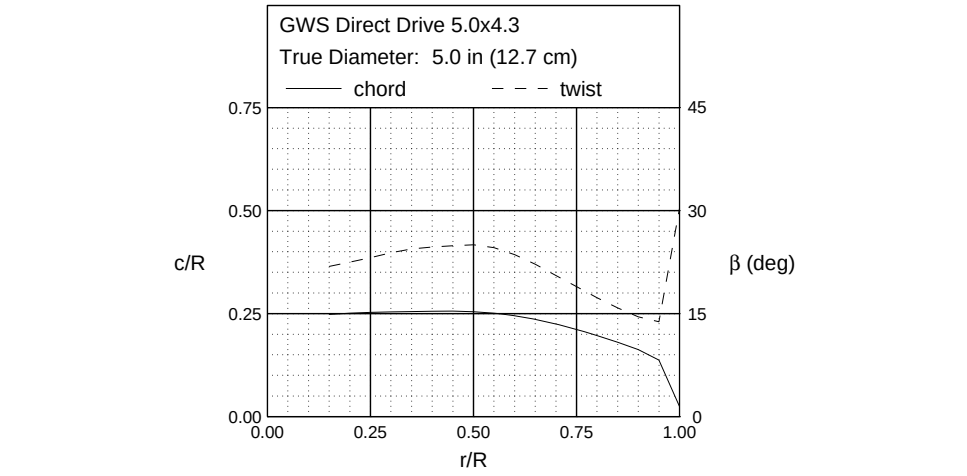

Front View

Side View

Figure 35. GWS Direct Drive 5.0×4.3 geometric characteristics.

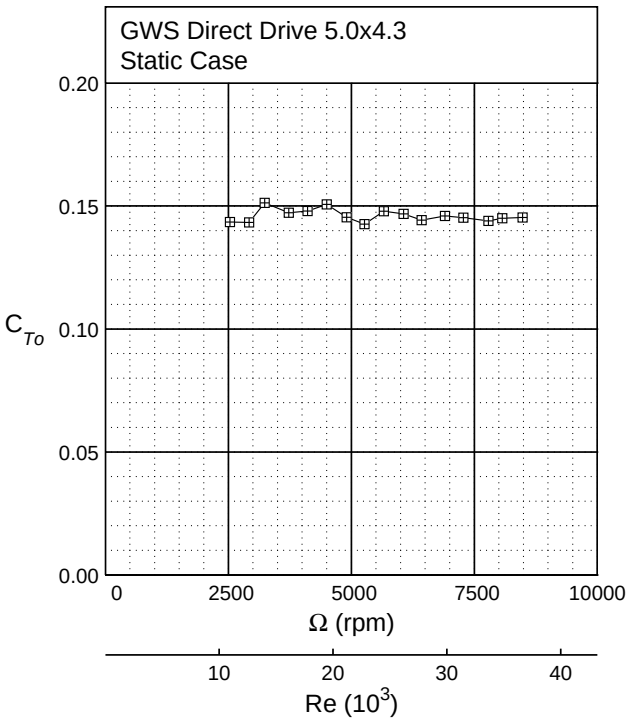

Figure 36. GWS Direct Drive 5.0×4.3 static thrust.

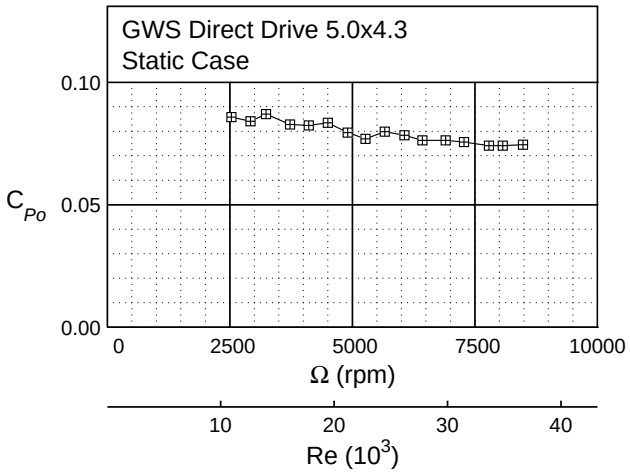

Figure 37. GWS Direct Drive 5.0×4.3 static power.

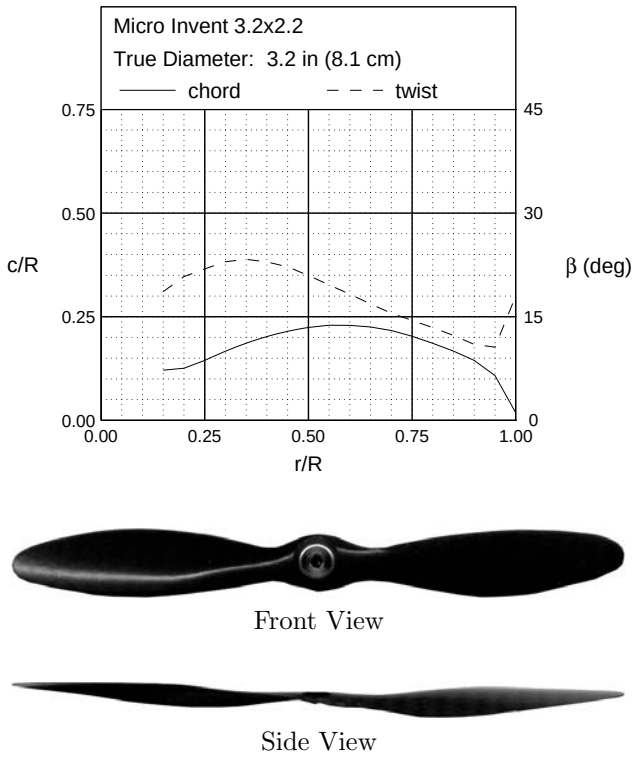

Figure 38. Micro Invent 3.2×2.2 geometric characteristics.

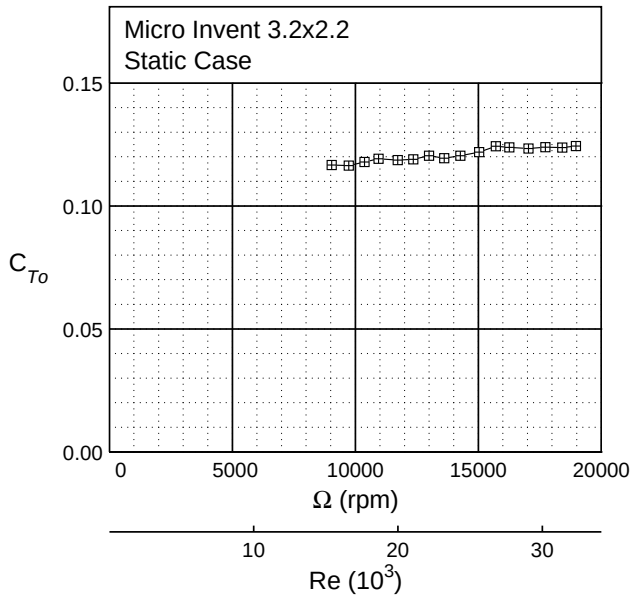

Figure 39. Micro Invent 3.2×2.2 static thrust.

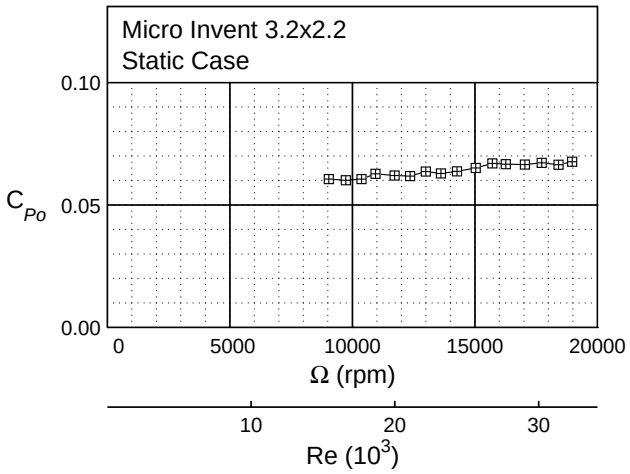

Figure 40. Micro Invent 3.2×2.2 static power.

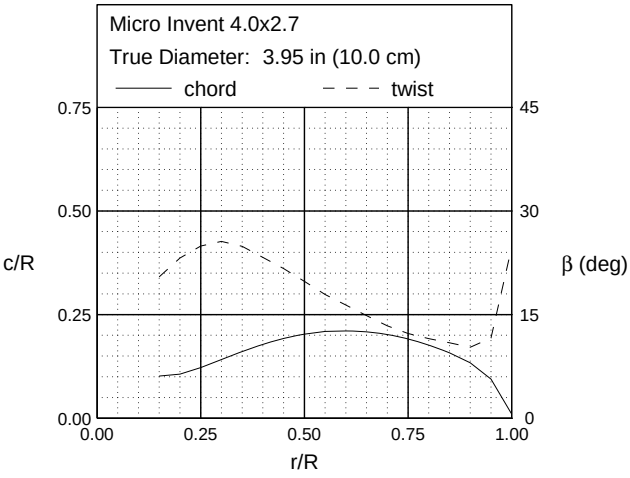

Front View

Side View

Figure 41. Micro Invent 4.0×2.7 geometric characteristics.

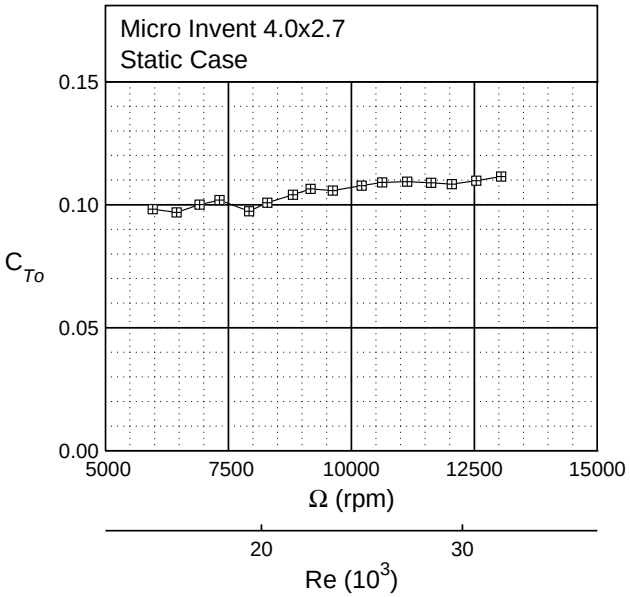

Figure 42. Micro Invent 4.0×2.7 static thrust.

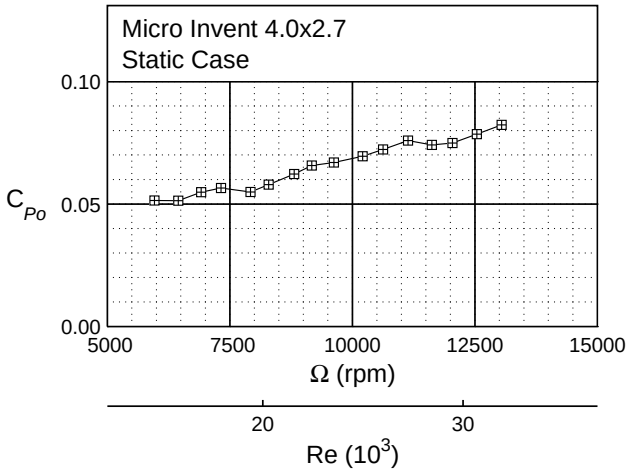

Figure 43. Micro Invent 4.0×2.7 static power.

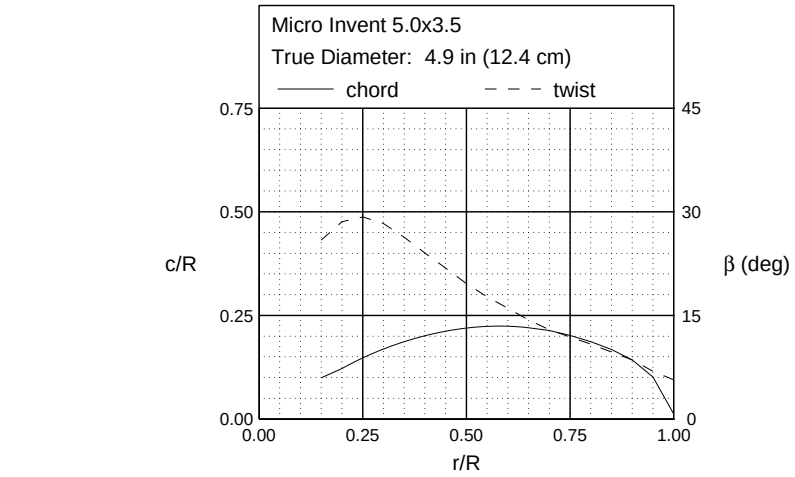

Front View

Side View

Figure 44. Micro Invent 5.0×3.5 geometric characteristics.

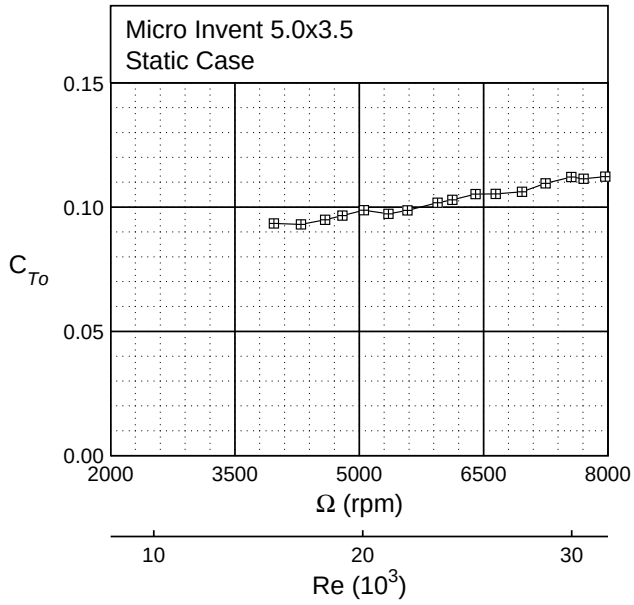

Figure 45. Micro Invent 5.0×3.5 static thrust.

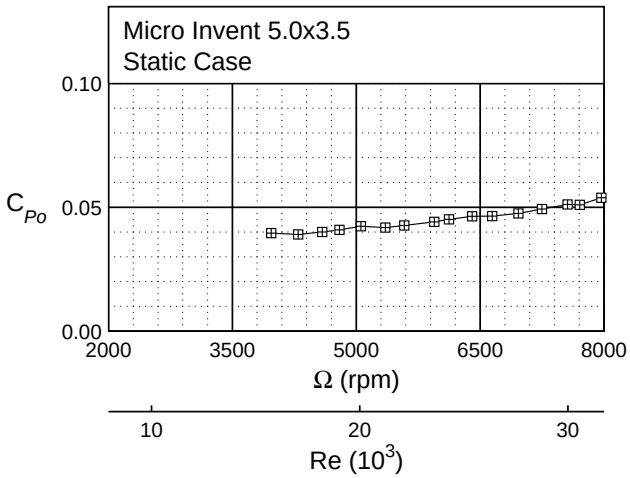

Figure 46. Micro Invent 5.0×3.5 static power.

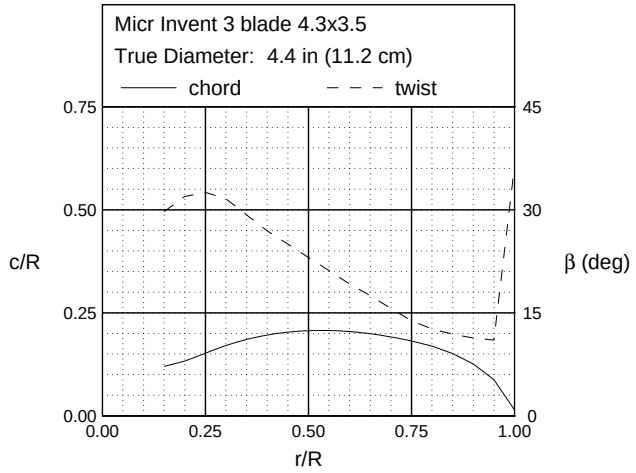

Front View

Side View

Figure 47. Micro Invent 3 blade 4.3×3.5 geometric characteristics.

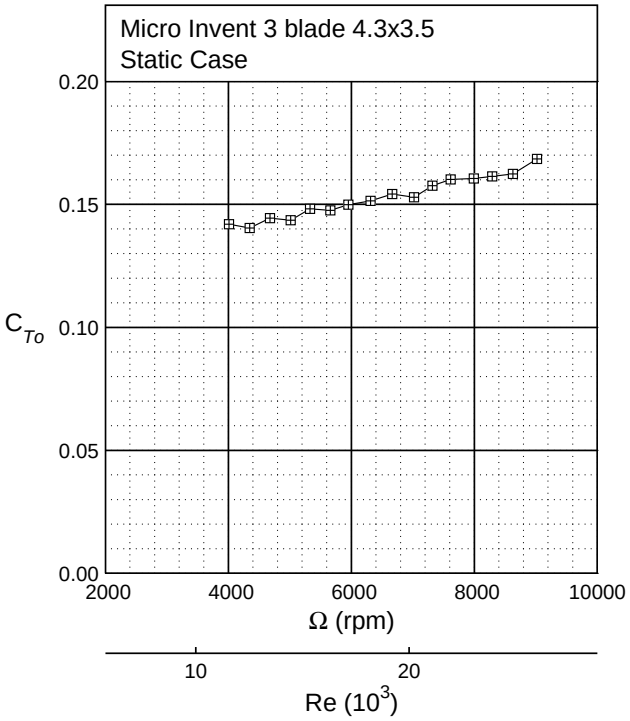

Figure 48. Micro Invent 3 blade 4.3×3.5 static thrust.

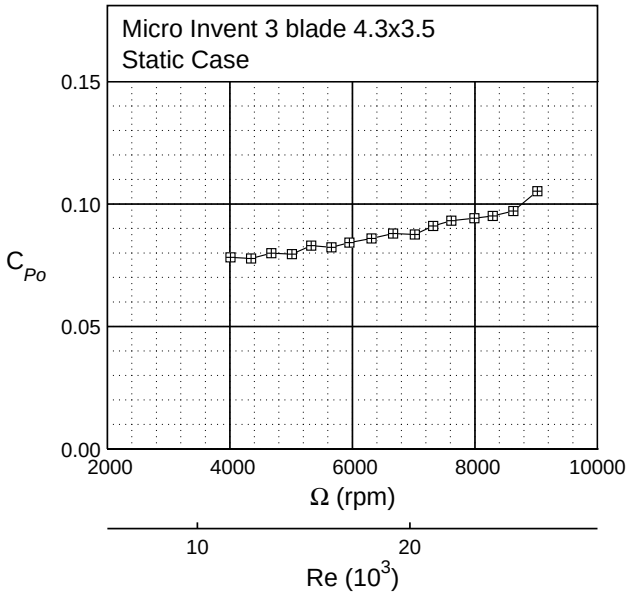

Figure 49. Micro Invent 3 blade 4.3×3.5 static power.

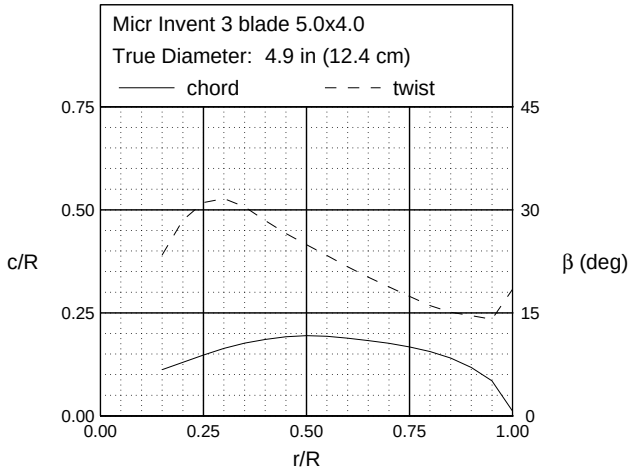

Front View

Side View

Figure 50. Micro Invent 3 blade 5.0×4.0 geometric characteristics.

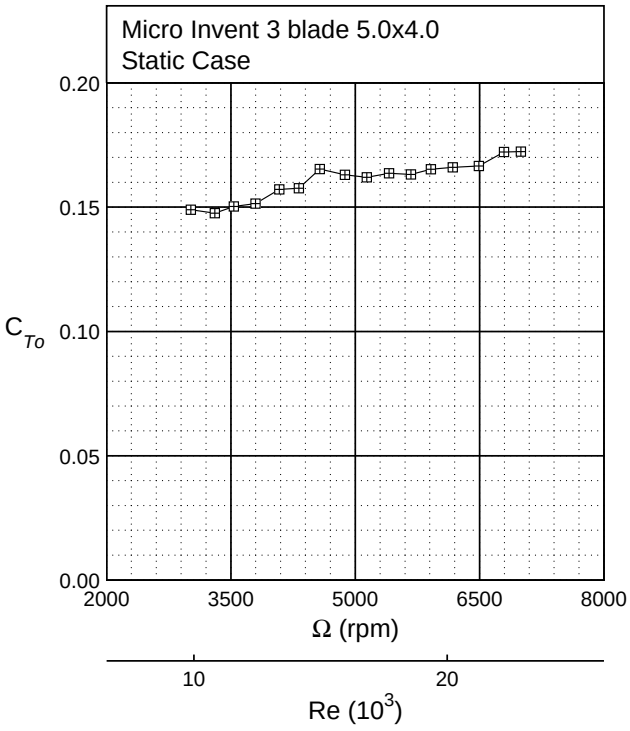

Figure 51. Micro Invent 3 blade 5.0×4.0 static thrust.

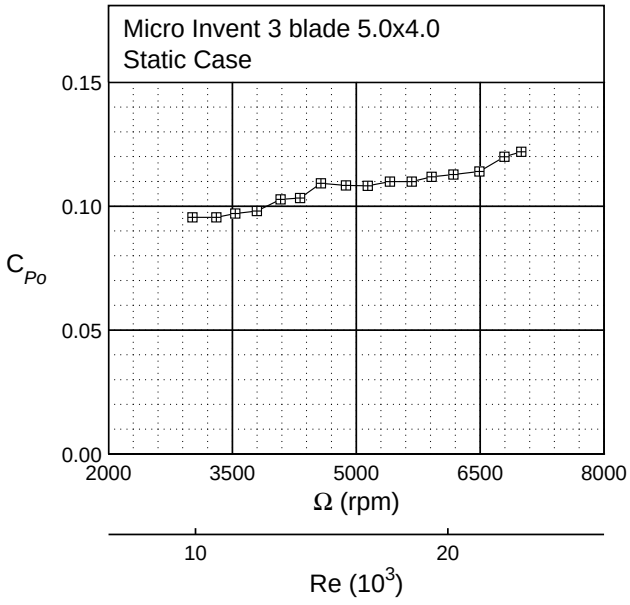

Figure 52. Micro Invent 3 blade 5.0×4.0 static power.

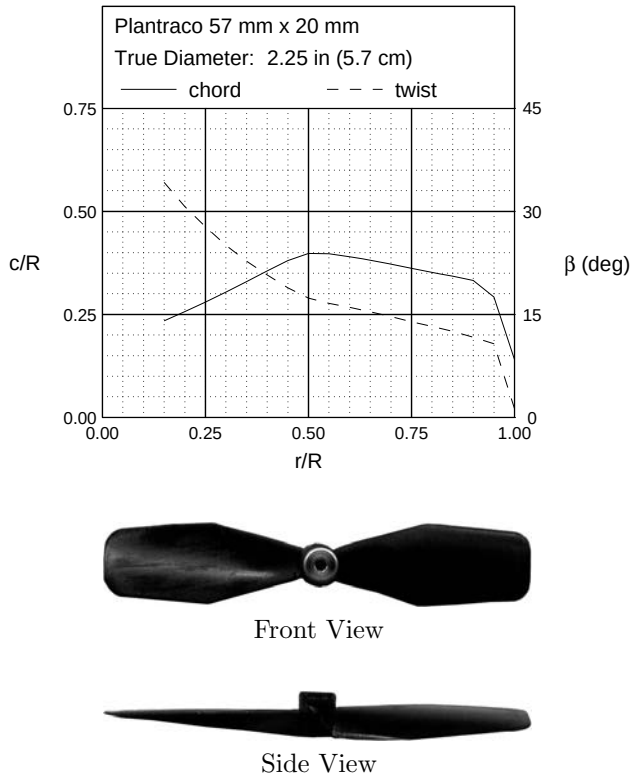

Figure 53. Plantraco 57 mm × 20 mm geometric characteristics.

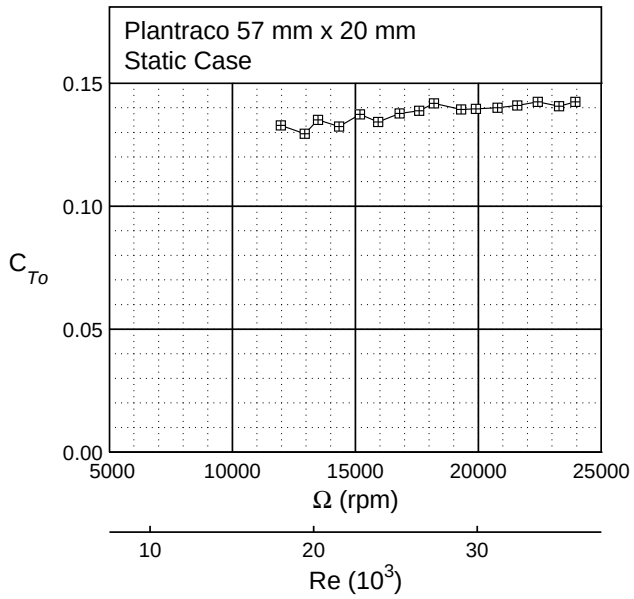

Figure 54. Plantraco 57 mm × 20 mm static thrust.

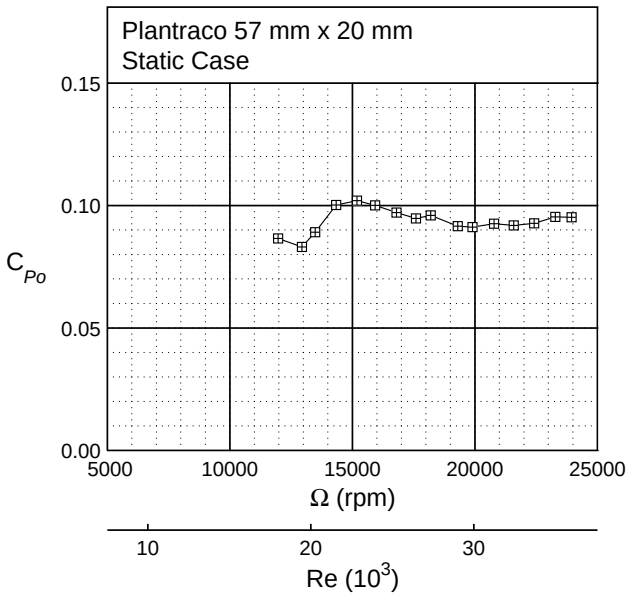

Figure 55. Plantraco 57 mm × 20 mm static power.

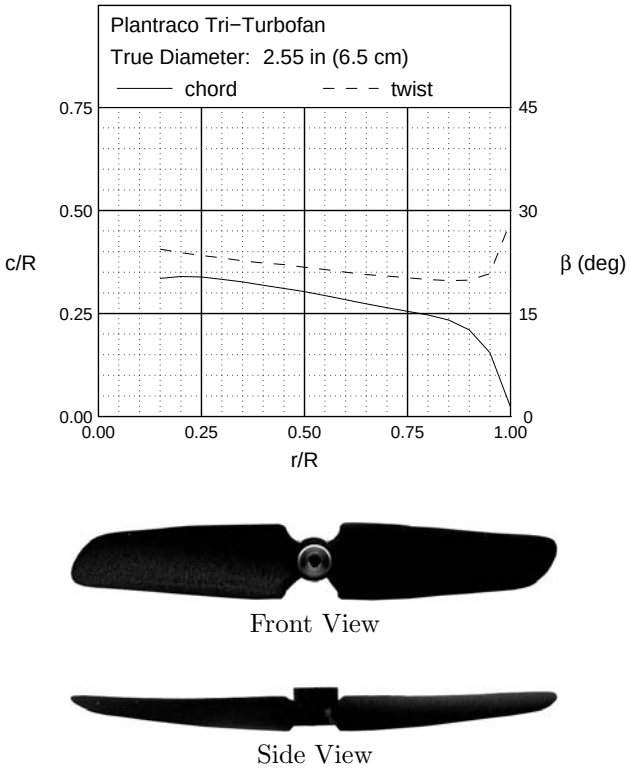

Figure 56. Plantraco Tri-Turbofan geometric characteristics.

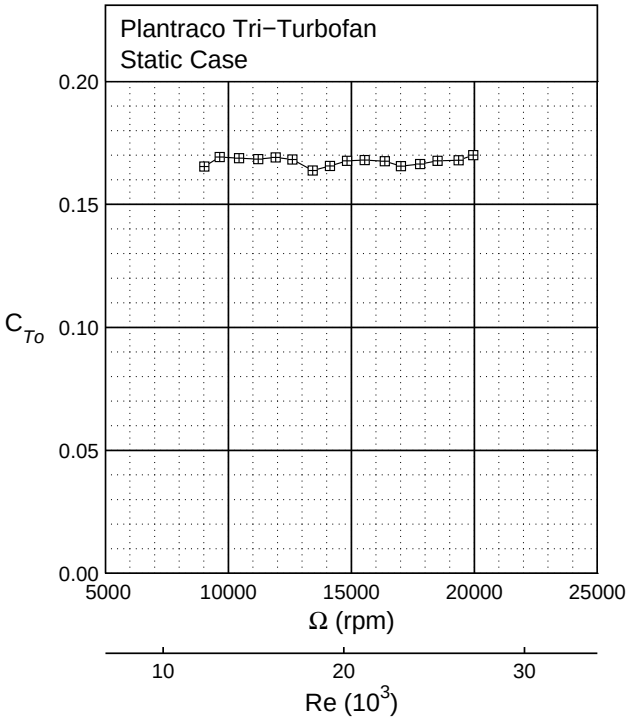

Figure 57. Plantraco Tri-Turbofan static thrust.

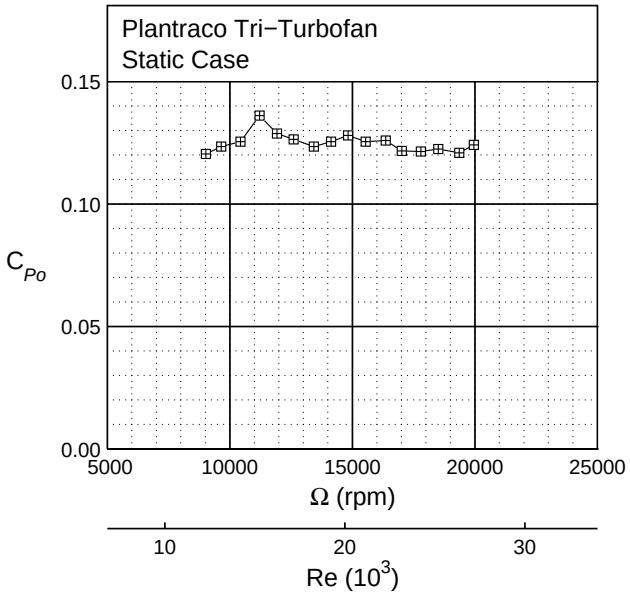

Figure 58. Plantraco Tri-Turbofan static power.

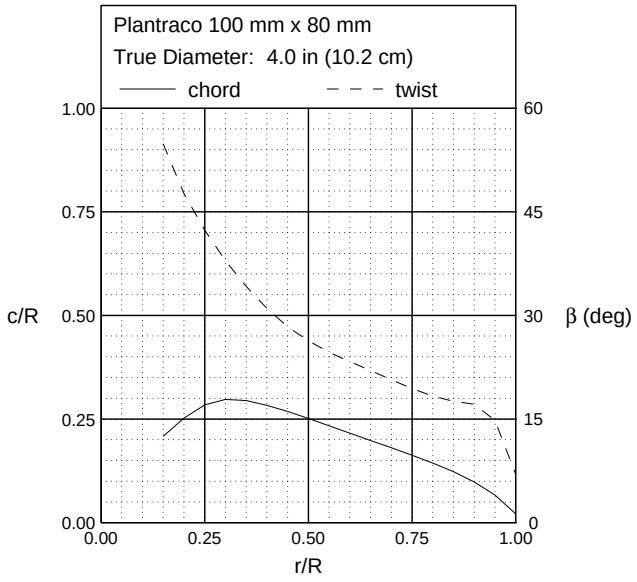

Front View

Side View

Figure 59. Plantraco 100 mm × 80 mm geometric characteristics.

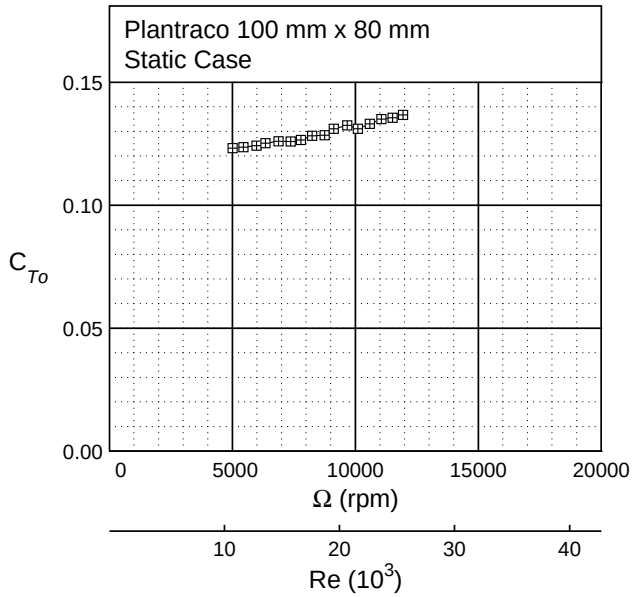

Figure 60. Plantraco 100 mm × 80 mm static thrust.

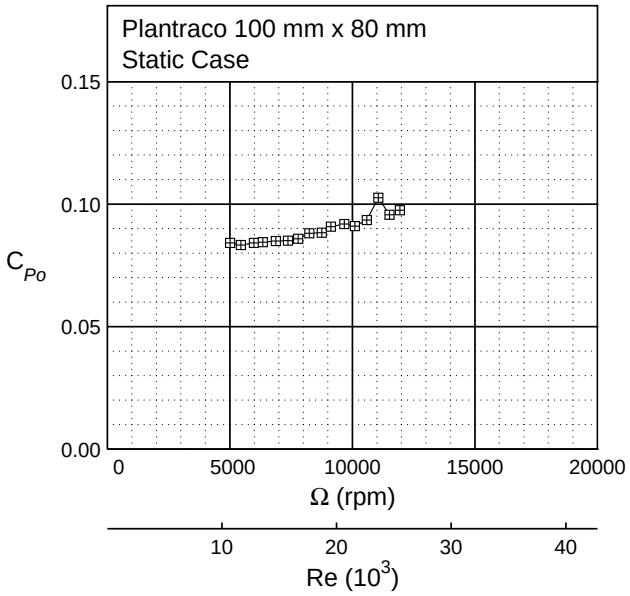

Figure 61. Plantraco 100 mm × 80 mm static power.

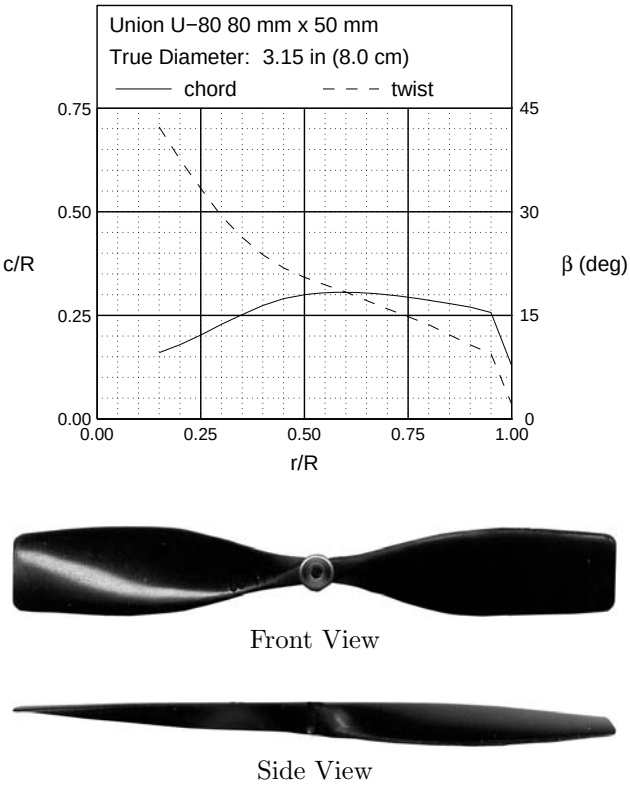

Front View

Side View

Figure 62. Union U-80 80 mm × 50 mm geometric characteristics.

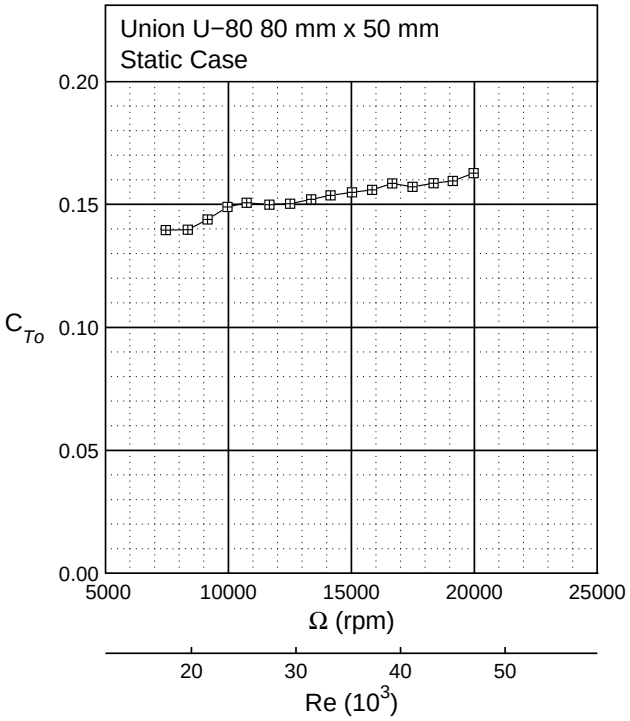

Figure 63. Union U-80 80 mm × 50 mm static thrust.

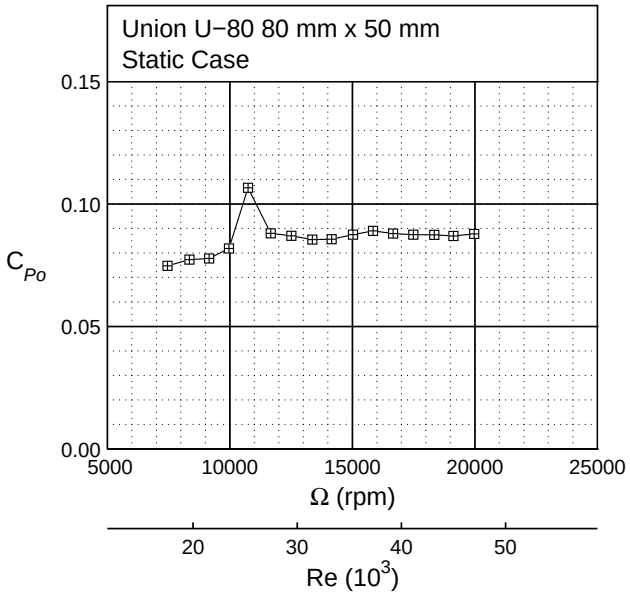

Figure 64. Union U-80 80 mm × 50 mm static power.

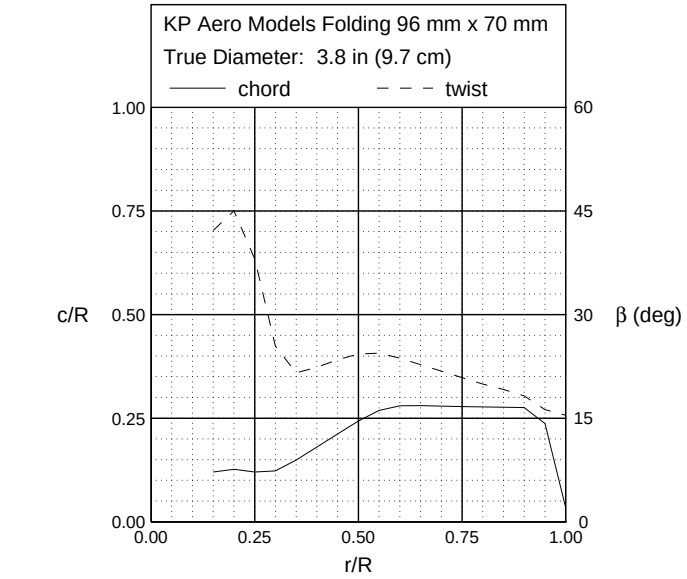

Front View

Side View

Figure 65. KP Aero Models Folding 96 mm × 70 mm geometric characteristics.

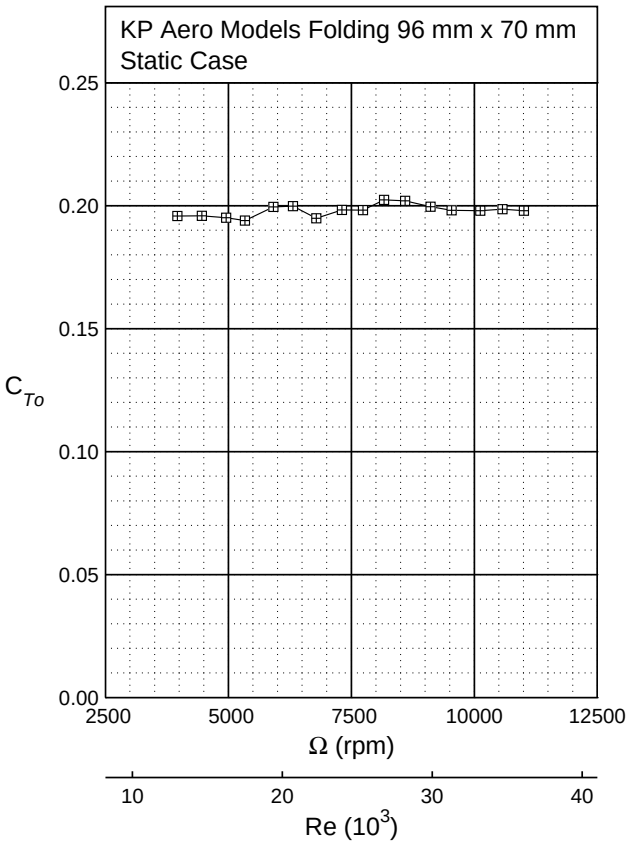

Figure 66. KP Aero Models Folding 96 mm × 70 mm static thrust.

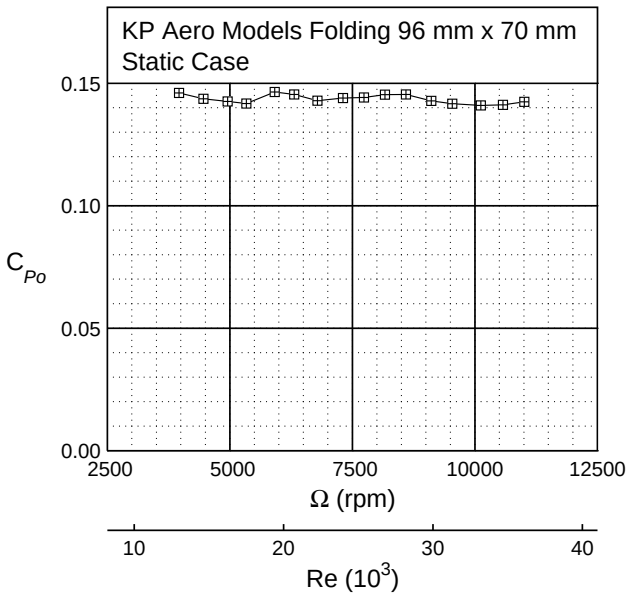

Figure 67. KP Aero Models Folding 96 mm × 70 mm static power.